

Radiation shielding properties of bismuth borate glasses doped with different concentrations of cadmium oxides



Y.S. Alajerami^{a,b,*}, D. Drabold^a, M.H.A. Mhareb^{c,d}, Katherine Leslee A. Cimatu^e, Gang Chen^a, M. Kurudirek^f

^a Physics and Astronomy, Science Faculty, Ohio University, USA

^b Medical Imaging Department, Applied Medical Sciences Faculty, Al Azhar University-Gaza, Palestine

^c Department of Physics, College of Science, Imam Abdulrahman Bin Faisal University, P.O. Box 1982, 31441, Dammam, Saudi Arabia

^d Basic and Applied Scientific Research Center, Imam Abdulrahman Bin Faisal University, P.O. Box 1982, 31441, Dammam, Saudi Arabia

^e Department of Chemistry and Biochemistry, Ohio University, 100 University Terrace, 136 Clippinger Laboratories, Athens, OH, USA

^f Department of Physics, Faculty of Science, Ataturk University, Turkey

ARTICLE INFO

Keywords:

Bismuth borate glass
Radiation shielding
Buildup factor
Neutrons

ABSTRACT

The current study is aimed to investigate the gamma ray and neutron shielding properties of the bismuth borate glass system with various concentration of cadmium oxide (0, 5, 10 and 15 mol%). The XRD spectra confirms the amorphous state of the prepared samples. A number of physical and mechanical properties (molar volume, oxygen molar volume, oxygen packing density, Poisson's ratio, optical absorption and dissolution rates) have been determined. The mass attenuation coefficients were estimated at different energy levels by using XCOM and EXABcal programs. The gamma and neutron beam shielding properties are evaluated through the calculation of several parameters such as equivalent number, specific gamma ray constant, gamma dose rate, specific absorbed fraction of energy and total neutron removal cross-section. Comparing with the standard gamma ray shielding materials, the new composition exhibits promising properties in terms of mass attenuation, halve value layer and mean free path. The glass with the highest concentration of CdO was found to be good shielding material for neutrons compared with some standard shielding materials (water, graphite, ordinary concrete and hematite-serpentine concrete).

1. Introduction

The using of ionizing radiation (electromagnetic and particle) in medical and industrial fields increases steadily. The benefits of these radiations are harnessed even more in electric power generation, medical diagnosis, radiotherapy, nuclear power and in many of the industrial processes. Several institutes and organizations have established guides for the safety use and deal with this type of radiation. The three cardinal principles of radiation protection are time, distance, and shielding [1]. The efficiency of shielding material can be improved by increase absorption of this material to the different types of ionizing radiation [2,3]. This principle can be classified into two types, structural and personal shielding. Concerning the structural shielding, two areas must be protected from ionizing radiation; the control panel area (the operator site) and the room walls to avoid external leakage of ionizing radiation [4,5]. For several years, lead and concrete were the best choice for shielding. These two materials exhibit some limitations

and problems (toxicity, opacity, installation difficulties and space consumption). Glass shielding is natural when transparent protection against ionizing radiation is essential [6]. Several studies have been conducted to show the efficiency of borate glass as an alternative for lead and concrete shielding [7–10]. The borate glasses show promising features in terms of the lowest melting point, transparency, and high thermal stability [11]. In order to improve radiation absorption performance of borate glass, heavy elements and oxides are included as modifiers to the borate-glass network. Among the different types of oxides, bismuth oxide shows excellent compatibility with borate glasses. Besides, it has a higher density and effective atomic number than lead (Pb) leading to improved radiation absorption, with less thickness [12–14]. Another candidate is cadmium oxide, which has high atomic number, high density, low binding energy and two different oxidation states [15,16].

Based on previous related studies, the attenuation efficiency of any proposed material can be classified into three main categories; gamma

* Corresponding author. Physics and Astronomy, Science Faculty, Ohio University, USA.

E-mail address: Yasser.s.alajerami@gmail.com (Y.S. Alajerami).

<https://doi.org/10.1016/j.ceramint.2020.02.039>

Received 18 December 2019; Received in revised form 27 January 2020; Accepted 5 February 2020

Available online 06 February 2020

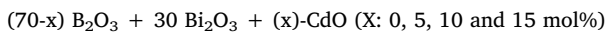
0272-8842/ © 2020 Elsevier Ltd and Techna Group S.r.l. All rights reserved.

ray-homogenous beam (narrow beam) shielding properties, gamma ray-heterogeneous beam (broad-beam) shielding properties and neutron shielding properties [17]. The shielding properties of the homogenous beam start with mass attenuation coefficient calculation and stop at the buildup factor (absorbance and exposure) which is related to heterogeneous beam shielding properties. Concerning fast neutron shielding properties, several calculation can be estimated to demonstrate material efficiencies such as removal cross-section, Σ_R (cm^{-1}), neutron scattering (coherent, incoherent and total) and absorption cross-section parameters. In the current study, the shielding properties of gamma-ray and neutron beam related to cadmium bismuth borate glasses in addition to some of significant physical and mechanical properties have been determined and will be discussed.

2. Material and methods

2.1. Experimental base

Based on melt-quenching techniques, bismuth-borate glasses with different concentrations of cadmium oxide (CdO) were prepared. Highly purified reagents (>99.5%) were weighed for 15g per batch and mixed mechanically for more than 3 h. The different concentrations of CdO were added based on the following stoichiometric equation:



The heating treatment used in this preparation was 900 °C (40–60 min) for melting and 450 °C (3 h) for annealing and finally cooling to room temperature with a cooling rate of 10 °C per minute.

The structure and optical properties of the prepared samples were investigated in the Lab Department of Physics and Astronomy of Ohio University-USA. The amorphous nature of the prepared samples was checked by using an X-ray Diffractometer (XRD) model Rigaku MiniFlex II. The Optical (UV–visible) absorption and transmission measurements were performed by using UV–Vis–NIR spectrometer (Agilent 8453).

The section glass durability or dissolution rate (*DR*) has been used to definite the resistance offered by a glass towards aqueous solutions and atmospheric agents [18]. In the current study, the durability of the prepared glasses was evaluated by immersing the glasses in jar filled with distilled water, then checked the weight of the glasses after specific time (2, 7 and 14 days). The dissolution rate was determined at room temperature based on the following expression [19]:

$$DR = \Delta\omega/At \quad (\text{g.cm}^{-2} \cdot \text{d}^{-1}) \quad (1)$$

where, $\Delta\omega$ is the weight change after glass immersion; *A* refers to the glass area and *t* is the immersion time.

2.2. Theoretical base

2.2.1. Gamma ray shielding properties

The expected interaction of narrow beam, has mono-energetic photons, with thin absorbing material is governed by the Lambert-Beer law:

$$I = I_0 \exp^{-\mu t} \quad (2)$$

where, I_0 is the intensity of incident photon, and *I* is the intensity of the same photon when it passes through absorbing material of thickness *t* and linear attenuation coefficient of μ . This equation will not be valid in case of broad-beam geometry in which case the equation turns out to be:

$$I = BI_0 \exp^{-\mu t} \quad (3)$$

B is a correction factor and is referred to as the *buildup factor* that used to correct the beam heterogeneity and material absorber thickness. $B > 1$, where the Lambert-Beer assumption does not apply otherwise will equal to 1. In other word, *B* is an expression for the ratio of the

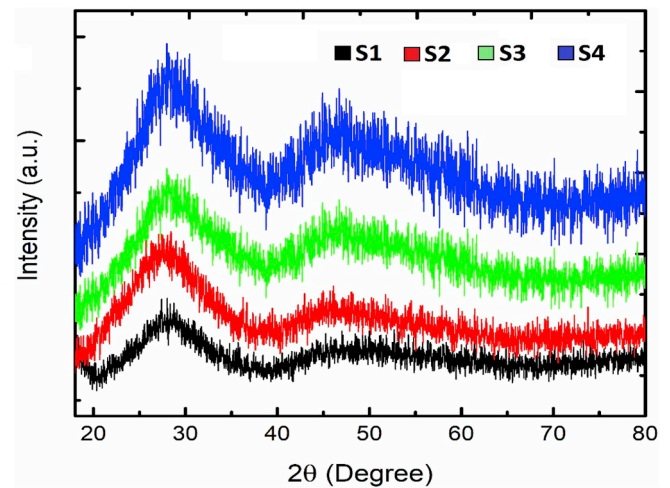


Fig. 1. XRD spectra of the prepared samples.

broad beam to the narrow beam. Based on the radiation interaction, *B* is divided to two types: (i) energy absorption buildup factor (EABF) and this correction is used when the deposited energy in the absorber or the detector system are of interest; (ii) exposure buildup factor (EBF) and this is related to the absorption obtained for detector and KERMA in air [20–22]. The buildup of the photon is an essential concept to evaluate the significance of secondary radiation for nuclear experiments, shielding design and absorbed dose estimation [17]. Basically, either EABF and EBF are photon energy and penetration depth-dependent. Photon attenuation coefficients are most often presented as atomic cross sections. The average distance that a photon/particle streams from the point of its emission to other point at which it creates its first interaction is called the mean-free-path length (mfp). Thus, the intensity of the incident photon is reduced by a factor of 1/*e* based on the number of used mfp.

The effective atomic cross-section (σ_{eff}) of the new glasses was calculated by using Eq. (4):

$$\sigma_{\text{eff}} = \frac{(\mu/\rho)_m}{N_A \sum_i \frac{w_i}{A_i}} \quad (4)$$

where $(\mu/\rho)_m$ is the mass attenuation coefficient of the sample, N_A is the Avogadro number, w_i is the weight fraction of the element and A_i refers to the atomic weight of each element in the composition.

One of the methods used to calculate *B* is the Geometric Progression (G-P) method. G-P is a fitting method that used to calculate EABF and EBF through the following three steps:

- Determining the equivalent atomic number (Z_{eq}).
- Evaluation of fitting parameters relies on the GP method.
- Estimation of EBF and EABF using different coefficients.

The Z_{eq} can be calculated by using the following equation:

$$Z_{\text{eq}} = \frac{Z_1(\log R_2 - \log R) + Z_2(\log R - \log R_1)}{\log R_2 - \log R_1} \quad (5)$$

where, *R* is the ratio of mass attenuation coefficient from the Compton interaction to the total interaction. The ratio of $(\mu_{\text{m Compton}}/\mu_{\text{m Total}})$ must be defined at a certain energy for a specific material. The value of *R* must be calculated between two adjacent elements Z_1 and Z_2 atomic number. R_1 and R_2 are the ratios of Compton scattering to the total interaction of the pure elements obtained from the WinXcom program [21,23].

In the second step, five different fitting parameters are required to evaluate the buildup factor by the G-P method. These coefficient parameters are provided by the American Nuclear Society (ANS) report

Table 1
Some of the physical and mechanical properties of the prepared glasses.

Sample Codes	Density (ρ) (g.cm ⁻³)	Molar volume (V_m) (m ³ .mol ⁻¹)	Oxygen Molar Volume (OMV) (cm ³ .mol ⁻¹)	Oxygen Packing Density (OPD) (g. atom.l ⁻¹)	Poisson's ratio (σ)	Number of Bonds per Unit Volume (N_b)
S1	4.315	46.689	14.563	68.667	0.229	6.893
S2	4.711	40.641	14.014	71.357	0.241	8.892
S3	5.068	38.358	13.699	72.996	0.249	9.421
S4	5.375	36.714	13.598	73.541	0.253	9.843

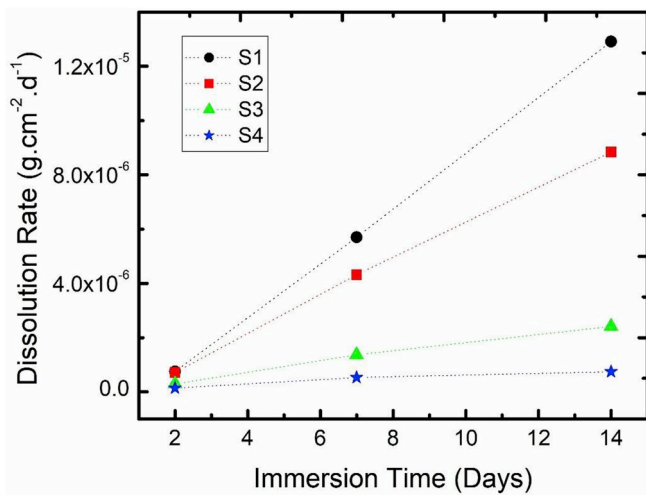


Fig. 2. Dissolution rates of the prepared glass for 14 days.

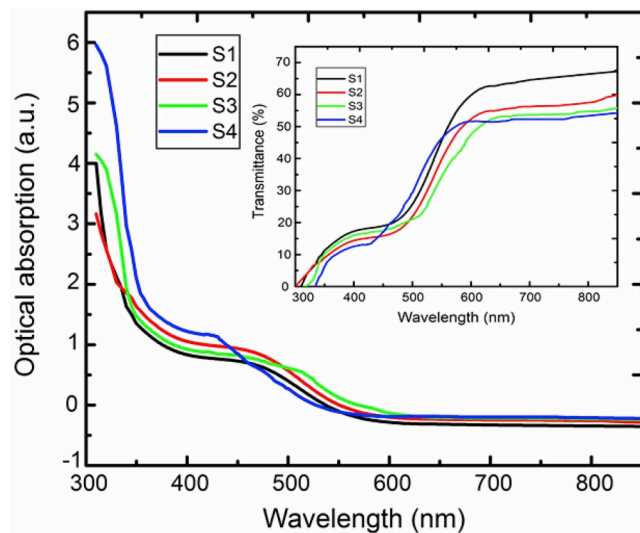


Fig. 3. The Optical absorption of all prepared glasses (Inset, corresponding transmission spectra) in the wavelength range 300–800 nm.

[24] for 23 elements and 25 standard photon energies. If there Ratio of the new composition does not match any of the 23 elements, the values of the G-P fitting parameters can obtain from following logarithmic interpolation formula:

$$P = \frac{F_1(\log Z_2 - \log Z_{eq}) + F_2(\log Z_{eq} - \log Z_1)}{\log Z_2 - \log Z_1} \quad (6)$$

where, F_1 and F_2 are the values of the G-P fitting coefficients corresponding to the elements with atomic numbers Z_1 and Z_2 respectively [24].

In the final step, the buildup factor is estimated at a specific energy and penetration depth (up to 40 mfp) by using the following

consequence equations (7)–(9):

$$B(E, x) = 1 + \frac{(b - 1)(K^x - 1)}{K - 1}, \text{ for } K \neq 1 \quad (7)$$

$$B(E, x) = 1 + (b - 1)x \text{ for } K = 1. \quad (8)$$

where,

$$K(E, x) = cx^a + d \frac{\tanh\left(\frac{x}{x_k} - 2\right) - \tanh(-2)}{1 - \tanh(-2)}, \text{ for } x \leq 40 \text{ mfp} \quad (9)$$

where, E, x , are the photon energy and the penetration depth (mfp) respectively. The other factors such as (c, a, d, x_k) are the G-P fitting parameters as clarified in Ref. [24].

Specific gamma ray constant (Γ) or gamma factor is the exposure rate (in R/hr) due to photons (E_γ) at a distance of 1 m from a source with the activity of 1 Ci can be computed based on the following equation [25]:

$$\Gamma = 657.68 X E_\gamma \left(\frac{\mu_{en}}{\rho} \right) \left(\frac{R. m^2}{Ci. hr} \right) \quad (10)$$

Based on the specific gamma ray constant (Γ), the dose (D) obtained in the glass network placed at a distance (r : in meters) from a radioactive source with activity (A : in Becquerels) at a time (t : in hours) can be estimated by the following expression:

$$D = \frac{\Gamma A t}{r^2} \quad (11)$$

The values of the energy absorption buildup factor (EABF) can be used to estimate the absorbed dose in a homogenous target. At a specific distance (x) between a radiation source and the target (glass sample), the specific absorbed fraction of the energy (SAFE) can be calculated based on the following equation [26]:

$$SAFE = \frac{\mu_{en} \exp(\mu\chi)(EABF)}{4\pi\chi^2\rho} (g-1) \quad (12)$$

where, μ_{en} is the linear absorption coefficient, x distance between radiation source and glass and ρ is the glass density.

2.3. Total Macroscopic cross section parameters

The removal cross-section (Σ_R) is the probability of a neutron collision in a specific homogenous material. The effective removal cross-section of the current glasses can be calculated based on the value of Σ_R for each element that is used to prepare the current glass mixture [26,27]:

$$\Sigma_R = \sum_i W_i (\Sigma_R/\rho)_i \quad (13)$$

where, W_i is the partial density of each element in the glass sample (g cm⁻³), Σ_R refers to the mass removal cross-section and ρ is the total sample density (g cm⁻³). In the current study, the effective removal cross-section was also determined by using the new friendly Phy-X program [28].

The shielding properties of a fast neutron in a condensed matter requires the calculation of both scattering length and absorption cross-sections of the constituent elements [29]. In the current study, the

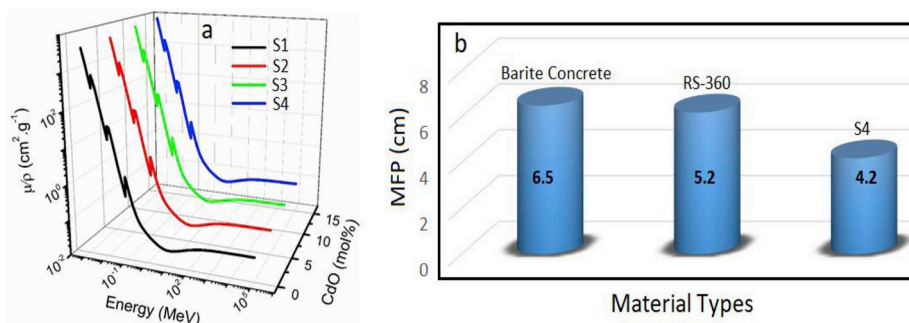


Fig. 4. (a)Variation of mass attenuation coefficient with photon energy for new glass samples, (b). comparison of the new prepared sample S4 with barite concrete and RS 360.

Table 2
Equivalent atomic number for the new glasses for energy region 0.015–15 MeV.

Energy (MeV)	S1		S2		S3		S4	
	Theo.	EXAB Cal						
0.015	20.38	20.66	21.00	21.24	21.43	21.82	21.94	22.35
0.02	24.24	24.99	25.04	25.37	25.48	25.76	25.91	26.2
0.03	25.80	26.22	27.49	27.88	28.98	29.46	30.47	31.25
0.04	26.64	27.26	28.34	28.91	29.91	30.75	31.55	32.44
0.05	27.28	28.08	28.97	29.86	30.53	31.65	32.76	33.25
0.06	27.80	28.76	29.49	30.44	31.02	32.36	34.06	34.89
0.08	28.63	29.09	30.27	31.51	31.83	32.41	41.03	41.82
0.1	47.52	48.12	48.23	48.86	49.08	49.58	51.11	51.87
0.15	49.55	50.12	50.16	51.09	50.84	51.21	52.11	52.52
0.2	50.73	51.09	51.35	52.59	51.99	52.52	53.00	53.88
0.3	52.17	53.88	52.47	53.37	53.49	54.17	54.75	55.65
0.4	52.94	53.13	53.49	54.51	54.03	55.12	55.21	56.33
0.5	53.27	54.62	54.04	55.27	54.49	55.93	56.22	57.49
0.6	53.79	54.22	54.31	55.91	54.81	55.44	56.51	57.96
0.8	54.01	54.46	55.2	56.41	56.03	57.94	57.11	58.46
1.0	54.26	55.08	54.76	55.6	55.55	56.31	56.61	57.63
1.5	51.93	52.19	52.47	53.81	53.05	54.44	53.89	54.37
2.0	43.89	44.33	44.97	45.39	43.45	44.80	47.43	48.12
3.0	32.09	32.32	33.62	34.03	35.29	35.76	36.95	37.49
4.0	27.5	27.87	29.34	29.59	31.13	31.66	32.99	33.15
5.0	25.57	25.71	27.33	27.88	29.15	29.72	30.97	31.29
6.0	24.52	24.88	26.29	26.32	28.13	28.88	29.62	30.06
8.0	23.37	23.91	25.09	25.39	26.87	26.93	28.14	28.78
10.0	22.85	23.03	24.56	24.89	26.32	27.14	27.81	28.28
15.0	22.45	22.58	24.15	24.27	25.92	26.22	27.33	27.72

neutron shielding properties (NPS) was expressed based on the following formula:

$$(NSP)_{compound} = \sum f_i (NSP)_i \tag{14}$$

where, f_i is the mass fraction of each element in the glass mixtures, and $(NSP)_i$ is the neutron shielding parameters of the i th element in the glass mixture [29]. In the current glass samples, the scattering lengths and the absorption cross-sections of the incident neutron determined by the following measurements:

- Coherent neutron scattering length (b_{coh}),
- Incoherent neutron scattering length (b_{inc}),
- Coherent neutron scattering cross-section (σ_{coh})
- Incoherent neutron scattering cross-section (σ_{inc})
- Total neutron scattering cross-section (σ_{tot})
- Neutron absorption cross-section (σ_{abs})

3. Results and discussion

3.1. Amorphous characterization

The amorphous nature of the prepared glasses was determined by using the X-ray Diffraction technique (XRD). Fig. 1 Shows broad peaks at 28° and 47° at 2θ angle, the spectra obtained from the measurement confirm the total amorphous structure of the prepared samples.

3.2. Physical and mechanical properties

Some of significant physical and mechanical properties of the prepared glasses are listed in Table 1. The calculated density showed a direct relation with the implemented percentage increment of CdO. The current enhancement is expected and attributed to the substitution of lighter compound (B_2O_3) by the heavier ones (CdO). The CdO has higher molecular weight and higher compound density compared to B_2O_3 . Oppositely, a reduction in the molar volume was reported with an increase of CdO. The indirect relation between density and molar volume gives an indication of glass compactness [30–32]. Based on that, we can assume that the increase in CdO content at the expense of B_2O_3 results to the opened glass network structure.

Also, it was observed that when B_2O_3 is substituted by CdO, the oxygen molar volume (OMV) values decreases from 14.563 to 13.598 $cm^3 mol^{-1}$. This reduction may be associated with a decrease in the number of oxygen atoms in the unit chemical composition. The oxygen packing density (OPD) is another parameter to explain the structure of prepared glasses. The calculated values show an increase in OPD with an increase of CdO from 68.667 $g.atom.l^{-1}$ to 73.541 $g.atom.l^{-1}$ for S1 and S4 respectively. The increase of OPD combined with the decrease of molar volume results to increase of mass density of the prepared glasses.

The Poisson ratios are < 0.3 which gives an indication of the high

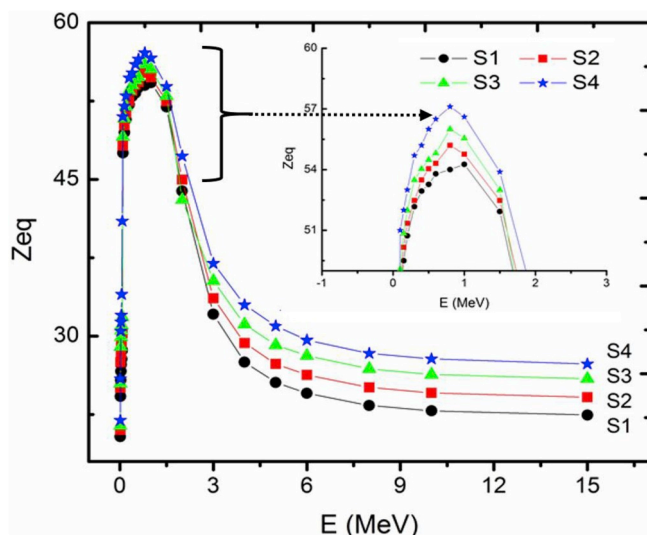


Fig. 5. The variation of Zeq with incident photon energy.

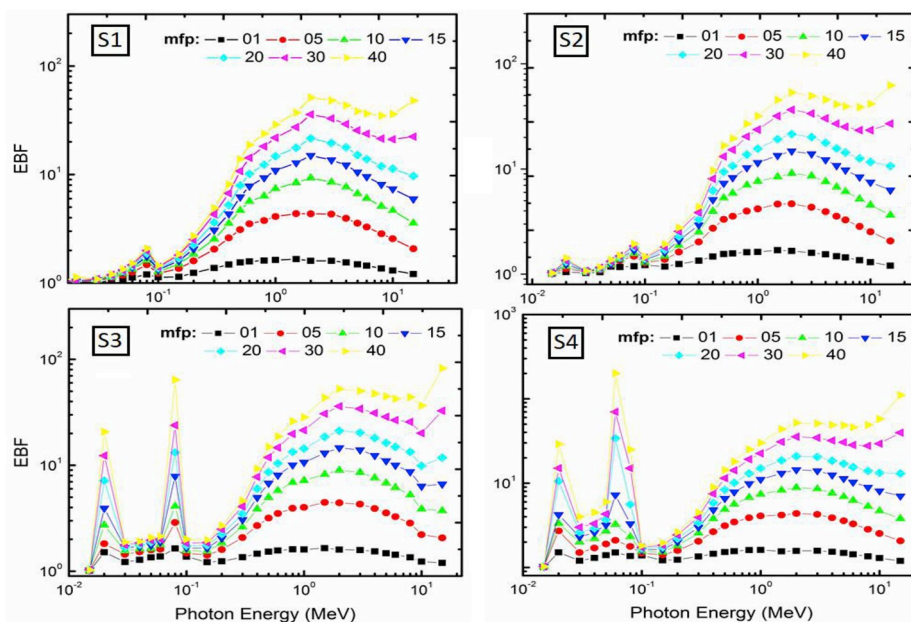


Fig. 6. Variation of EBF values as a function of photon energy for different CdO mol%.

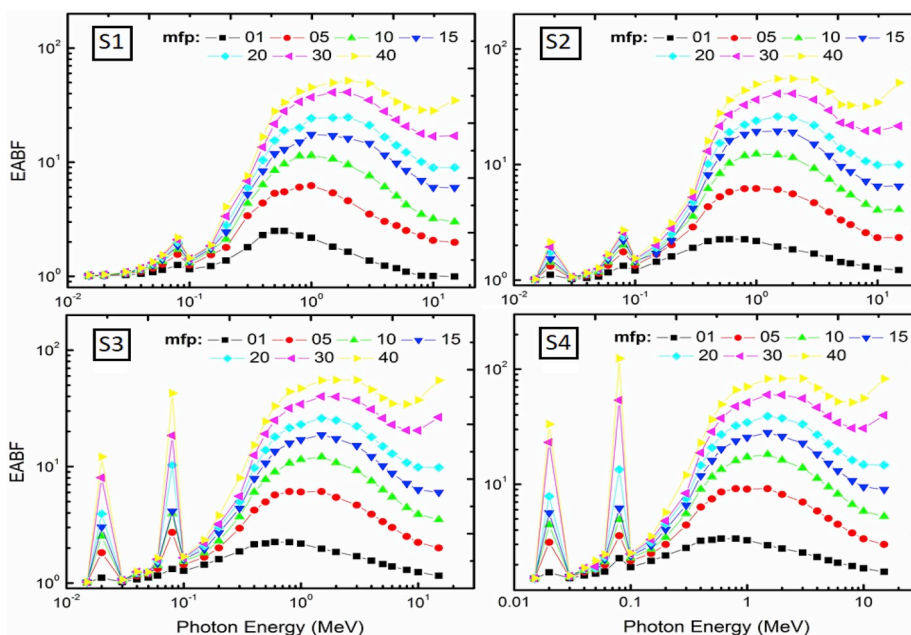


Fig. 7. Variation of EABF values as a function of photon energy for different CdO mol%.

cross-linking density of the prepared glasses. Furthermore, an increase in the value of Poisson's ratio as a function of CdO concentration indicates that an equal amount of stress was applied throughout the glass composition and the lateral strain was gradually leveled out [33]. The number of bonds per unit volume shows remarkable enhancement from 6.893 to $9.843 \times 10^{28} \text{ m}^{-3}$ that is due to the high coordination number of CdO [CdO₆].

3.3. Glass durability

Fig. 2 shows an increase in the DR with increasing immersion time, and this is highly expected to the possibility of ion exchange and hydration inside the glass network [18,34]. Obviously, the DR had decreased gradually from 7.523×10^{-7} to $1.415 \times 10^{-7} \text{ g.cm}^{-2}.\text{d}^{-1}$ due to an increase in CdO content. This current result proved the ability of

CdO to reduce hygroscopic of the bismuth-borate glass and improved the water-resistance of the prepared glasses.

3.4. Optical properties

The transparency of the current glasses was evaluated by using UV-Vis-NIR Agilent 8453 absorption spectrophotometer in the wavelength region of 200 nm to 900 nm. Fig. 3 illustrates that all prepared glass has good visible light transmission (>50% from 550-850 nm).

3.5. Radiation shielding properties

The mass attenuation coefficient (μ_m) of the prepared glasses was determined based on the weight fraction of the compounds used to create the glass mixture by applying the following formula:

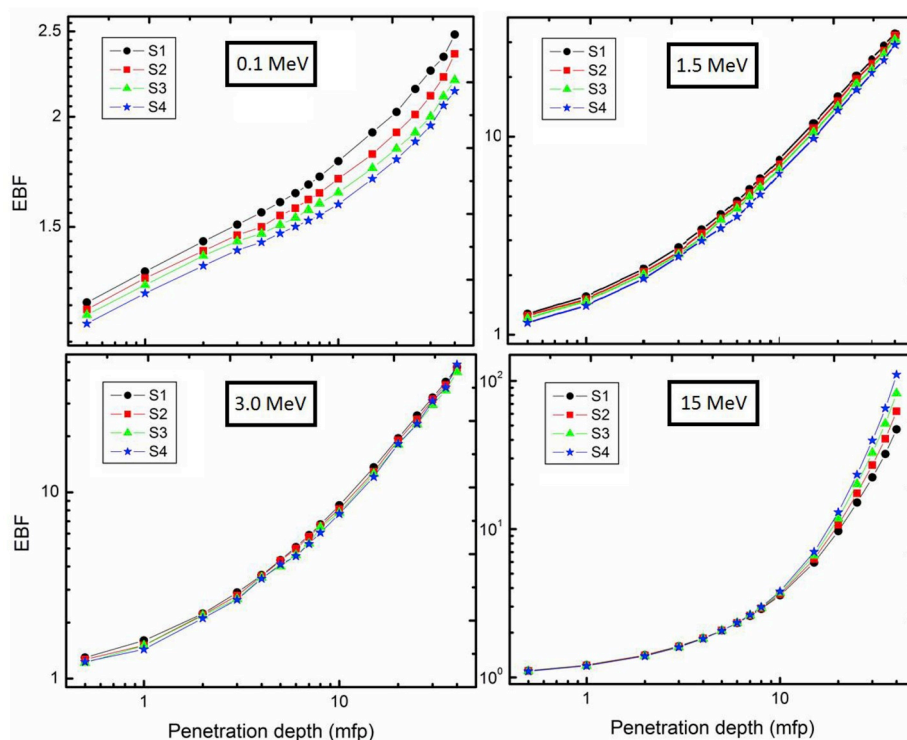


Fig. 8. Exposure buildup factor for all prepared glasses with penetration depths at specific photon energies.

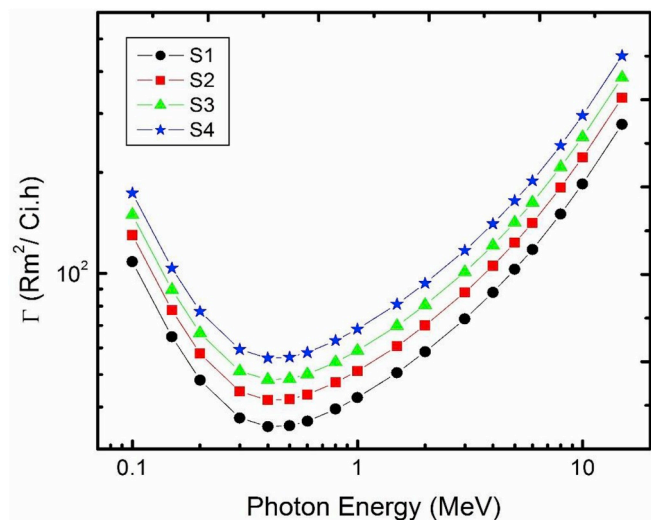


Fig. 9. Variation of the specific gamma ray constants for the new glasses at different energies.

$$\mu_m = \sum_i w_i \mu_{m,i} \tag{15}$$

where, w_i is the compounds' weight fraction (B_2O_3 , Bi_2O_3 and CdO) and μ_m is the mass attenuation coefficient of the mixture obtained by using XCOM and EXABCal software [35]. Basically, the mass attenuation coefficient increase with increasing density of composition and decrease with increasing energy of an incident photon. Fig. 4 demonstrates the relation between the new prepared glasses and a wide range of photon energy (0.01 to 15 MeV). A sharp decrease in the attenuation coefficient was reported with the continuous increasing of photon beam energy. At intermediate energy level (150 keV to 5 MeV), the reduction became slow then started to increase reaching a constant response. This trend refers to the different interaction possibilities of photon with the material (photoelectric, Compton and pair production). Concerning to

the three sharp peaks observed in this pattern, the peaks at 0.004 and 0.2 MeV refer to the L- and K-absorption edges of the CdO compound [36], and the peak at 0.09 MeV refer to the K-absorption edge of Bi [34]. Also, it is noted that by increasing the CdO concentration the interaction between the incident photon and the prepared glasses increases. Simply, the increment of CdO increases the glass density and this leads to an increase interaction and consequently, the release of electrons via photoelectric effect or Compton scattering. Consequently, S4 has the highest μ_m value and the number of absorbed photons in this sample will be the highest compared to the other samples. Compare with the standard shielding materials (Barite concrete and RS 360), 35% shortness in the Mean Free Path (MFP) was achieved with S4 (show Fig. 4b).

The equivalent atomic number (Z_{eq}) for the new glass systems was estimated by the Geometric Progression (G-P) method [37–39] and by using the friendly computer software EXABCal [35]. The recording values are obtained from the mass attenuation coefficient estimated by using the XCOM program. The equivalent atomic number can be represented as the average weighted electron per atom for the whole composition. Eventually, the radiation interaction properties of the composition can be described based on the interaction probabilities.

Computation of the Z_{eq} of the current glasses for total photon interaction has been estimated using Eq. (4). Table 2 shows great compatibility between the calculated values of Z_{eq} and that obtained by using the online software Phy-X [28]. The values show a direct relation between CdO content and Z_{eq} as shown in Fig. 5 (S4 has the highest Z_{eq}). This trend is highly expected due to increase glass density by replacement of a small atomic number of boron with high atomic number element such as Cd. The sharp peak observed at low energy level is ascribed to the K- and L-absorption edges of Cd, which is clearly enhanced by increasing of CdO concentration.

The values of the exposure buildup factor (EBF) and energy absorption buildup factor (EABF) were also determined as a function of penetration depth (mfp) for all prepared glasses at wide energy range (0.015–15 MeV) as shown in Fig. 6 and Fig. 7. Generally, both of EBF and EABF are increased with increasing of penetrating depth, but the

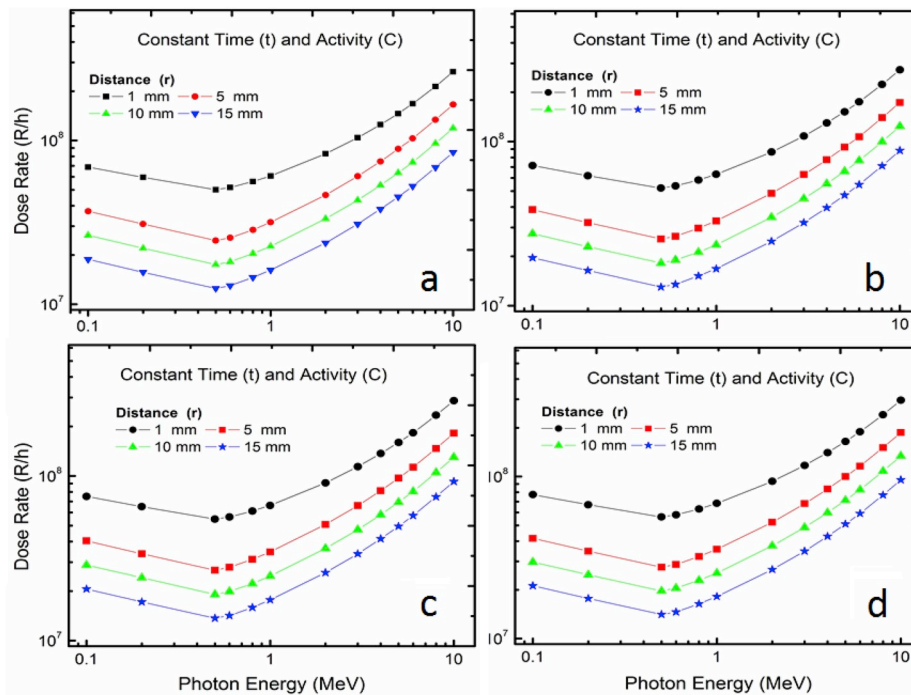


Fig. 10. Variations of gamma dose rate at different energy levels for the prepared glasses.

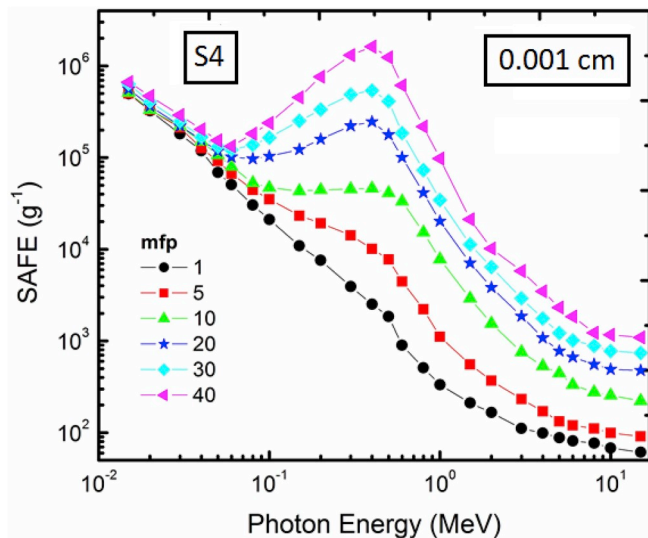


Fig. 11. The variation of SAFE with incident photon energy for S4 at 0.001 cm for various mfps.

effect of CdO was varied and reported as energy-dependent:

- At low energy level (<0.1 MeV), the values of buildup factor for exposure and absorption are the lowest and this refers to the abundance of the photoelectric effect and a sharp peak at the level of 0.09 MeV is ascribed to the K-absorption edge of Bi (this peak was observed in all observed glasses). Another peak was reported at 0.2 MeV with starting the increment of CdO (S2–S4), which is clearly related to the K-absorption edge of Cd [36].
- At intermediate energy level (0.1–10 MeV), both EBF and EABF increase with increase energy and raised to the maximum value at 1.5 MeV that is expected to high possibilities of Compton scattering effect.
- At very high energy level (>10 MeV), the values had a tendency to gradually increase by increasing incident energy due to the pair

Table 3

The removal cross-sections and mass removal cross-section of the prepared glasses.

Sample Code	Element	Mass fraction	Weight Fraction	Partial Density P (g cm ⁻³)	Removal Cross Section Σ _R (cm ⁻¹)	
					Manual Calculation	Using Phys-X
S1	B	0.080	0.217	0.936	0.103	0.094
	O	0.253	0.514	2.218		
	Bi	0.667	0.269	1.161		
S2	B	0.074	0.202	0.952	0.109	0.100
	O	0.241	0.485	2.285		
	Cd	0.030	0.044	0.207		
S3	Bi	0.655	0.269	1.267	0.115	0.105
	B	0.067	0.186	0.943		
	O	0.230	0.457	2.316		
S4	Cd	0.058	0.087	0.441	0.122	0.108
	Bi	0.645	0.270	1.368		
	B	0.061	0.171	0.919		
	O	0.218	0.429	2.306		
	Cd	0.085	0.131	0.704		
	Bi	0.636	0.269	1.446		

production phenomenon. The current results agreed with previous related studies [40–42]. The probability of pair production in photon–matter interactions increases with photon energy and increases approximately as the square of atomic number. Consequently, the buildup of secondary gamma photons generated by electron-positron annihilation in the medium due to multiple scattering events. In addition, the increase in penetration depth of the materials leading to increase the thickness of the interacting material which in turn leads to increase the scattering events in the interacting medium, in particular for the material with the highest equivalent atomic number (such as Cd in this study). Hence it results in large EABF and EBF values [43,44].

Fig. 8 illustrates the EBF values at different energies (0.1, 1.5, 3 and 15 MeV). At 0.1 MeV, it can clearly observe the EBF variations between the prepared glasses (S1–S4) and these variations are reduced by

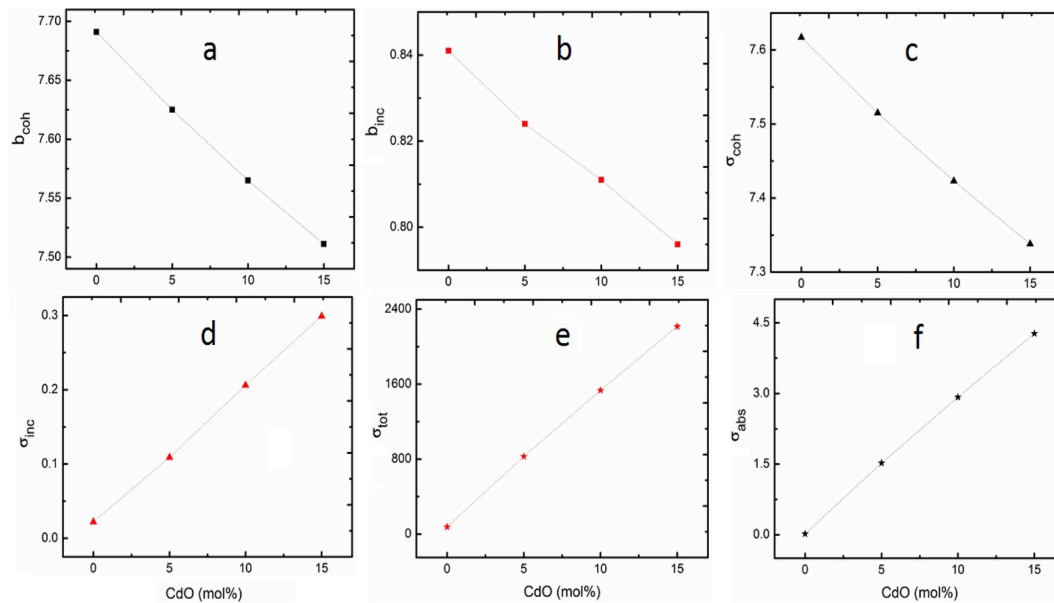


Fig. 12. The neutron scattering and absorption parameters for new prepared samples (b_{coh} : the coherent neutron scattering length, b_{inc} : the incoherent neutron scattering length, σ_{coh} : the coherent neutron scattering cross-section, σ_{inc} : the incoherent neutron scattering cross-section, σ_{tot} : the total neutron scattering cross-section, σ_{abs} : the absorption neutron scattering cross-section).

increasing the energy as shown at 1.5 MeV. This variation ascribed to the different concentrations of CdO, which means, the EBF depends on the glass composition and reduce by increasing the CdO mol%. At 3 MeV, the EBF values become independent of the composition of the glass matrix. The same trend was remarked at 15 MeV with little variation at high penetrating depth (> 10 mfp). According to Fig. 6, 7 and 8, the glass with a high concentration of CdO (15 mol%) has the highest equivalent atomic numbers and the lowest EBF and EABF values [36,45].

The variation of the specific gamma ray constants for the new glasses at different energies is shown in Fig. 9. In the low energy level (0.1 up to 0.4 MeV) the variation of the specific gamma ray constant decreased in all prepared glasses (predominant of absorption effect) then starts to increase gradually with increasing of incident photon energy (predominant of scattering effect and penetrating power). The effect of CdO on the trend of the specific gamma ray is obvious, in which the glass with the highest CdO content got the highest constant [46].

Fig. 10 shows the variations of gamma dose rate (R/hr) at different energy levels with different thicknesses (1, 5, 10 and 15 mm) for the prepared glasses. The gamma dose rate was reduced with increasing the energy from 0.1 MeV to 0.5 MeV, then gradually increased with increasing photon energy. Generally, the gamma dose rate decreased with increasing thickness of glass thickness. Also, the effect of CdO is clear that the gamma dose rate was the highest with the glass contains the highest CdO (S4).

The specific absorbed fraction of the energy (SAFE) up to 40 mfp at a 0.001 cm thickness in S4 was shown in Fig. 11. The obtained results show an increase in the SAFE values up to (0.4 MeV) and then decrease. The maximum value of SAFE at this energy level is ascribed to the crossing or matching between the photoelectric interaction coefficients and Compton scattering interaction coefficients, which directly depends on the glass composition and density. At this energy level, the Compton scattering exceeds, which leads to high scattering events that starting from partial to full absorption. Regarding the low and high energy levels, the SAFE values reduced due to the dominance of photoelectric effect and pair production phenomena respectively. As expected, the minimum SAFE values reported at the high energy levels (dominant of pair production) in which the possibility of reduced specific absorption [36].

The removal cross-section of the fast neutron was determined by calculation (Eq. (12)) and by using the friendly program Phys-X (Table 3). The values are very close and showed the same trend by increasing the CdO content. Both of removal cross-section and mass removal cross-section are increased by increasing the CdO content and the highest value is 0.122 cm^{-1} for glass sample S4, which is better compared to some standard shielding materials (water = 0.102 cm^{-1} , graphite = 0.077 cm^{-1}), and concrete (ordinary = 0.094 cm^{-1} , hematite-serpentine = 0.097 cm^{-1}) [47,48]. This can be attributed to the increment and spontaneous increasing of Cd weight fraction at the expense of B and O. In addition, the mass removal cross-section (Σ_R/ρ) of Cd is larger than B and O as shown in Table 3.

Fig. 12 shows the number of neutron shielding parameters (NSP) that were estimated for the new. Obviously, the values of b_{coh} , b_{inc} and σ_{coh} decreased with increasing of CdO content. On the contrary, the absorption neutron scattering cross-section (σ_{abs}) increased with increasing of CdO. The NSP attained by S4 are ($b_{coh} = 7.511 \text{ fm}$; $b_{inc} = 0.796 \text{ fm}$; $\sigma_{coh} = 7.338 \text{ b}$ and $\sigma_{abs} = 4.272 \text{ b}$). The material with these properties is expected to be potential candidate for neutron shielding applications [44].

4. Conclusion

A new glass system of bismuth-borate with different concentration of cadmium oxide was prepared and proposed for radiation shielding applications. The current results revealed an improvement in the network stability and chemical durability with the increment of CdO. The gamma and neutron shielding properties such as μ_m , Z_{eq} , SAFE, EBF, b_{coh} , b_{inc} , σ_{coh} and σ_{abs} of the new glasses have estimated at different energy levels. The results exhibited the improvement of shielding properties with increasing of CdO content. The MFP new glass exhibits around 35% and 19% shorter between successive collisions in that obtained with barite concrete and RS-360. Regarding the fast neutron effective removal cross-section, the glass with 15 mol% of CdO (S4) has $\Sigma_R = 0.122 \text{ cm}^{-1}$, which is higher than some standard shielding materials (water = 0.102 cm^{-1} , graphite = 0.077 cm^{-1}), and concrete (ordinary = 0.094 cm^{-1} , hematite-serpentine = 0.097 cm^{-1}). This new glass composition is a good and an improved shielding material that can be used in various radiation protection applications (personal and structural).

Acknowledgment

The authors would like to gratefully acknowledge the Institute of International Education (IIE)/Fulbright program (2019/2020) and Nanoscale & Quantum Phenomena Institute for their financial support and also for the use of the services and facilities of Ohio University. DAD and GC thank the NSF under grant DMR-1507670.

References

- J.H. Kim, Three principles for radiation safety: time, distance, and shielding, *Korean.J.Pain.* 31 (3) (2018) 145.
- James E. Martin, Chul Lee, Principles of Radiological Health and Safety, first ed., John Wiley Sons, Inc., Hoboken, New Jersey, 2003.
- A.N. Kim, Y.J. Chang, B.K. Cheon, J.H. Kim, How effective are radiation reducing gloves in C-arm fluoroscopy-guided pain interventions? *Korean.J.Pain.* 27 (2) (2014) 145.
- National council on Radiation protection and measurements, Radiation Protection in Dentistry, NCRP Report No. 145, NCRP, Bethesda, MD, 2003.
- IAEA Safety Standards, Radiation Protection and Safety in Medical Uses of Ionizing Radiation vol. 46, IAEA SAFETY STANDARDS SERIES, No. SSG-, VIENNA, 2018.
- E. Kavaz, N.Y. Yorgun, Gamma ray buildup factors of lithium borate glasses doped with minerals, *J. Alloys Compd.* 752 (5) (2018) 61–76.
- M.G. Dong, M.I. Sayyed, G. Lakshminarayana, M. Çelikkbilek Ersundu, A.E. Ersundu, Priyanka Nayar, M.A. Mahdi, Investigation of gamma radiation shielding properties of lithium zinc bismuth borate glasses using XCOM program and MCNP5 code, *J. Non-Cryst. Solids* 468 (2017) 12e16.
- A.M.A. Mostafa, Shams A.M. Issa, M.I. Sayyed, Gamma ray shielding properties of PbO-B₂O₃-P₂O₅ doped with WO₃, *J. Alloys Compd.* 708 (2017) 294e300.
- M.I. Sayyed, Saleem I. Qashou, Z.Y. Khattari, Radiation shielding competence of newly developed TeO₂-WO₃ glasses, *J. Alloys Compd.* 696 (2017) 632e638.
- M. Parandamaiah, K.N. Kumar, S. Babu, S.V.R. Reddy, Y.C. Ratnakaram, Dy³⁺ doped lithium sodium bismuth borate glasses for yellow luminescent photonic applications, *Int. J. Eng. Res. Afr.* 5 (2015) 126e131.
- D.D. Ramteke, K. Annapurna, V.K. Deshpande, R.S. Gedam, Effect of Nd³⁺ on spectroscopic properties of lithium borate glasses, *J. Rare Earths* 32 (2014) 1148e1153.
- N. Singh, et al., Comparative study of lead borate and bismuth lead borate glass systems as gamma-radiation shielding materials, *Nucl. Instrum. Methods Phys. Res., Sect. B* 225 (3) (2004) 305–309.
- K. Kaur, K. Singh, V. Anand, Structural properties of Bi₂O₃-B₂O₃-SiO₂-Na₂O glasses for gamma ray shielding applications, *Radiat. Phys. Chem.* 120 (2016) 63–72.
- A. Saeed, Y. Elbasha, Optical properties of high density barium borate glass for gamma ray shielding applications, *Opt. Quant. Electron.* 48 (1) (2016) 1–10.
- R.M.M. Morsi, M.A.F. Basha, M.M. Morsi, Synthesis and physical characterization of amorphous silicates in the system SiO₂-Na₂O-RO (R = Zn, Pb or Cd), *J. Non-Cryst. Solids* 439 (2016) 57–66.
- R. Kaur, S. Singh, O.P. Pandey, Influence of CdO and gamma irradiation on the infrared absorption spectra of borosilicate glass, *J. Mol. Struct.* 1049 (2013) 409–413.
- Murat Kurudirek, Photon buildup factors in some dosimetric materials for heterogeneous radiation sources, *Radiat. Environ. Biophys.* 53 (2014) 175–185.
- A. Paul, Chemical durability of glass, *Chemistry of Glasses*, Springer, Dordrecht, 1982, p. 108.
- L. Koudelka, et al., Structure and properties of barium niobophosphate glasses, *J. Non-Cryst. Solids* 459 (2017) 68–74.
- I.O. Olarinoye, Photon buildup factors for tissues and phantom Materials for penetration depth up to 100 mfp, *J. Nucl. Res. Dev.* 13 (2017) 57–67.
- Y. Harima, An historical review and current status of buildup factor calculations and application, *Radiat. Phys. Chem.* 41 (4/5) (1993) 631–672.
- M.I. Sayyed, M.Y. AlZaatareh, M.G. Dong, M.H.M. Zaid, K.A. Matori, H.O. Tekin, A comprehensive study of the energy absorption and exposure buildup factors of different bricks for gamma-ray shielding, *Results in Phys* 7 (2017) 2528–2533.
- K.S. Mann, T. Korkut, Gamma-ray buildup factors study for deep penetration in some silicates, *Ann. Nucl. Energy* 51 (2013) 81–93.
- AMSL/ANS-6.4.3, Gamma Ray Attenuation Coefficient and Buildup Factors for Engineering Material, American Nuclear Society, La Grange Park, Illinois, 1991.
- H.C. Manjunatha, L. Seenappa, B.M. Chandrika, Chikka Hanumantharayappa, A study of photon interaction parameters in barium compounds, *Ann. Nucl. Energy* 109 (2017) 310–317.
- M.F. Kaplan, Concrete Radiation Shielding, John Wiley and Sons., New York, USA, 1989.
- J. Wood, Computational Methods in Reactor Shielding, Pergamon Press, Inc., New York, USA, 1982.
- E. Sakar, O. Firat, B. Alim, M.I. Sayyed, M. Kurudirek, Phys-X/PSD: development of a user friendly online software for calculation of parameters relevant to radiation shielding and dosimetry, *Radiat. Phys. Chem.* 166 (2020) 108496.
- V.F. Sears, Neutron scattering lengths and cross section, *Neutron News* 3 (3) (1992) 26–37.
- M.H.A. Mhareb, S. Hashim, S.K. Ghoshal, Y.S.M. Alajerami, M.A. Saleh, M.M.A. Maqableh, N. Tamchek, Optical and erbium ion concentration correlation in lithium magnesium borate glass, *Optik* 126 (23) (2015) 3638–3643.
- M.H.A. Mhareb, Almessiere Ma, M.I. Sayyed, Y.S.M. Alajerami, Physical, structural, optical and photons attenuation attributes of lithium-magnesium-borate glasses: role of Tm²⁺ doping, *Optik* 182 (2019) 821–831.
- V. Dimitrov, S. Sakka, Electronic oxide polarizability and optical basicity of simple oxides, *Int. J. Appl. Phys.* 79 (3) (1996) 1736.
- M.H.M. Zaid, K.A. Matori, L.C. Wahetal, Elastic moduli prediction and correlation in soda lime silicate glasses containing ZnO, *J. of Inter. Phys. Sci.* 6 (2011) 1404–1410.
- Parminder Kaur, K.J. Singh, Murat Kurudirek, Sonika Thakur, Study of environment friendly bismuth incorporated lithium borate glass system for structural, gamma-ray and fast neutron shielding properties, *Spectrochim. Acta Mol. Biomol. Spectrosc.* 223 (2019) 117309.
- I.O. Olarinoye, R.I. Odiaga, S. Paul, EXABCal: a program for calculating photon exposure and energy absorption buildup factors, *Heliyon* 5 (2019) e02017.
- B. YasserSaddeek, A.M. Shamsissa, T. Alharbi, K. Aly, Mahmoud Ahmad, H.O. Tekin, Mechanical and nuclear shielding properties of sodium cadmium borate glasses: impact of cadmium oxide additive, *Ceram. Int.* 46 (3) (2020) 2661–2669.
- M. Kurudirek, Photon buildup factors in some dosimetric materials for radiation sources, *Radiat. Environ. Biophys.* 53 (2014) 175–185.
- M. Dong, X. Xue, A. Kumar, H. Yang, M.I. Sayyed, S. Liu, E. Bu, A novel method of utilization of hot dip galvanizing slag using the heat waste from itself for protection from radiation, *J. Hazard Mater.* 344 (2018) 602–614.
- V.P. Singh, N.M. Badiger, Energy absorption buildup factors, exposure buildup factors and Kerma for optical stimulated luminescence materials and their tissue equivalence for radiation dosimetry, *Radiat. Phys. Chem.* 104 (2014) 61–67.
- S. Gupta, G.S. Sidhu, Energy absorption buildup factor for some oxide glasses: penetration depth, *Photon Energy and Effective* 2 (2012) 1–7.
- G. Lakshminarayana, S.O. Baki, A. Lira, M.I. Sayyed, I.V. Kityk, M.K. Halimah, M.A. Mahdi, X-ray photoelectron spectroscopy (XPS) and radiation shielding parameters investigations for zinc molybdenum borotellurite glasses containing different network modifiers, *J. Mater. Sci.* 52 (2017) 7394–7414.
- M.I. Sayyed, G. Lakshminarayana, Structural, thermal, optical features and shielding parameters investigations of optical glasses for gamma radiation shielding and defense applications, *J. Non-Cryst. Solids* 487 (2018) 53–59.
- M.G. Dong, R. El-Mallawany, M.I. Sayyed, H.O. Teking, Shielding properties of 80TeO₂-5TiO₂-(15-x)WO₃-xAnOm glasses using WinXCom and MCNP5 code, *Radiat. Phys. Chem.* 141 (2017) 172–178.
- M.I. Sayyed, H. Elhouichet, Variation of energy absorption and exposure buildup factors with incident photon energy and penetration depth for boro-tellurite (B₂O₃-TeO₂) glasses, *Radiat. Phys. Chem.* 130 (2017) 335–342.
- H.O. Tekin, O. Kılıcoglu, E. Kavaz, E.E. Altunsoy, M. Almatari, O. Agar, M.I. Sayyed, The investigation of gamma-ray and neutron shielding parameters of Na₂O-CaO-P₂O₅-SiO₂ bioactive glasses using MCNPX code, *Results Phys* 12 (2019) 1797–1804.
- H.C. Manjunatha, L. Seenappa, B.M. Chandrika, K.N. Sridhar, Chikka Hanumantharayappa, Gamma, X-ray and neutron shielding parameters for the Al-based glassy alloys, *Appl. Radiat. Isot.* 139 (2018) 187–194.
- V.P. Singh, N. Badiger, Shielding efficiency of lead borate and nickel borate glasses for gamma rays and neutrons, *Glas. Phys. Chem.* 42 (3) (2015) 276–283.
- A. El Abd, et al., A simple method for determining the effective removal cross section for fast neutrons, *J. Radiat. Nucl. Appl.* 2 (2) (2017) 53–58.